

## Carbon and nitrogen export during the JGOFS North Atlantic Bloom Experiment estimated from $^{234}\text{Th}$ : $^{238}\text{U}$ disequilibria

KEN O. BUESSELER,\* MICHAEL P. BACON,\* J. KIRK COCHRAN†  
and HUGH D. LIVINGSTON\*

(Received 5 December 1990, in revised form 13 September 1991, accepted 26 November 1991)

**Abstract**—The disequilibrium between the particle-reactive tracer  $^{234}\text{Th}$  ( $t_{1/2} = 24.1$  days) and its soluble parent,  $^{238}\text{U}$ , was used to examine Th scavenging and export fluxes during the U.S. JGOFS North Atlantic Bloom Experiment (24 April–30 May 1989) at  $\sim 47^\circ\text{N}$ ,  $20^\circ\text{W}$ . Four profiles of dissolved and particulate  $^{234}\text{Th}$  in the upper 300 m and a non-steady state box model were used to quantify dissolved  $^{234}\text{Th}$  uptake and particle export rates. The highest export fluxes occurred during the first half of May. From  $\text{POC}/^{234}\text{Th}$  and  $\text{PON}/^{234}\text{Th}$  ratios, particulate organic C and N fluxes were calculated. Results were  $5\text{--}41 \text{ mmol C m}^{-2} \text{ day}^{-1}$  and  $0.9\text{--}6.5 \text{ mmol N m}^{-2} \text{ day}^{-1}$  from the 0–35 m layer. The ratio of POC export flux to primary production ranged from 0.05 to 0.42, peaking in the first half of May. The estimated fluxes agree with the observed losses of total C and N from the upper ocean during the bloom, but yield significantly higher fluxes than were measured by floating traps at 150 and 300 m.

### INTRODUCTION

BIOLOGICAL activity in the surface ocean is important for its role in the uptake and export of carbon and nutrients. Surface water productivity also is thought to be a driving force behind a wide range of processes, such as the scavenging of trace metals, mid-water feeding and respiration, deep-ocean sedimentation and early diagenesis. Due to the natural complexity and seasonality in the biological driving forces, the links between surface biota and these geochemical processes can be variable in space and time. For example, the flux of particles from surface waters to the deep sea can show strong seasonal variability due to changes in surface productivity and food web structure (McCAYE, 1984, DEUSER, 1986, FOWLER and KNAUER, 1986, MICHAELS and SILVER, 1988, PEINERT *et al.*, 1989). Likewise, the ratio of carbon export to carbon uptake in surface waters (the 'f-ratio') is variable (EPPLEY and PETERSON, 1979, PLATT and HARRISON, 1985, HARRISON *et al.*, 1987, EPPLEY, 1989).

In studies of the cycle of carbon and associated elements in the surface ocean, it would be useful if the complex biological system could be reduced to simple terms which provide a measure of the seasonal or daily averaged rates of carbon or nutrient uptake and export.  $^{234}\text{Th}$  is an appropriate tracer for quantifying particle formation and export rates in the surface ocean on time scales of days to weeks due to its particle reactive chemistry, simple

---

\*Woods Hole Oceanographic Institution, Woods Hole, MA 02543, U.S.A.

†Marine Sciences Research Center, State University of New York, Stony Brook, NY 11794-5000, U.S.A.

source term from  $^{238}\text{U}$ , and half-life of 24.1 days (SANTSCHI *et al.*, 1979; KAUFMAN *et al.*, 1981; COALE and BRULAND, 1985, 1987, BRULAND and COALE, 1986) EPPLEY (1989) proposed that if the particles to which Th adsorbs are biogenic, then  $^{234}\text{Th}$  and particulate carbon data could be used to estimate new production. This hypothesis was based upon the inverse relationship found by COALE and BRULAND (1985) between the residence time of dissolved  $^{234}\text{Th}$  and primary production.

This paper provides a closer look at using  $^{234}\text{Th}$ : $^{238}\text{U}$  disequilibria to estimate particle fluxes by examining data collected during the U.S. JGOFS (Joint Global Ocean Flux Study) North Atlantic Bloom Experiment (NABE). The samples were collected from late April through May of 1989 at approximately 47°N, 20°W. Time-series data were collected for the application of a non-steady state model of  $^{234}\text{Th}$  scavenging. Using this model we estimate  $^{234}\text{Th}$  uptake and removal rates, and by comparison to particulate carbon and nitrogen data, estimate C and N export fluxes. These estimates are independent of the fluxes that were measured directly with floating sediment traps and can be compared with them.

## SAMPLING AND ANALYSES

### *Measurement of $^{234}\text{Th}$ at sea*

In order to monitor changes in  $^{234}\text{Th}$  as the bloom progressed, we developed a procedure to measure this isotope at sea. This technique employs a gamma detector to measure  $^{234}\text{Th}$  activities from large volume samples (1000–4000 l) collected with *in situ* pumps (WINGET *et al.*, 1982, SACHS *et al.*, 1989). Particulate  $^{234}\text{Th}$  is collected on a 0.5  $\mu\text{m}$  nominal pore size polypropylene cartridge filter (CUNO Microwynd DPPPZ) and dissolved  $^{234}\text{Th}$  is collected with two  $\text{MnO}_2$  impregnated adsorbers (LIVINGSTON and COCHRAN, 1987). Although  $^{234}\text{Th}$  can be measured with higher sensitivity by beta counting (sample sizes of 60–200 l—BHAT *et al.*, 1969, COALE and BRULAND, 1985), the larger samples allowed for a considerable simplification of the  $^{234}\text{Th}$  analyses. The large volumes also were required for the radiochemical analyses of the longer-lived isotopes which are being measured as part of this project ( $^{238}\text{Th}$ ,  $^{230}\text{Th}$ ,  $^{232}\text{Th}$  and  $^{231}\text{Pa}$ ). The details of this procedure are described in BUESSELER *et al.* (1992).

As this was our first experience with the at-sea  $^{234}\text{Th}$  analyses, the method was altered slightly to improve the precision from  $\pm 10$  to 15% on NABE leg 2 (R/V *Atlantis II*) to 5% or better on leg 3 (BUESSELER *et al.*, 1992). The error reported for  $^{234}\text{Th}$  is propagated from the one sigma counting uncertainty and errors due to detector calibration, background corrections, and, for dissolved  $^{234}\text{Th}$ , the error associated with the calculation of the  $\text{MnO}_2$  cartridge collection efficiency. The accuracy of our total analytical procedure is demonstrated by the finding of total  $^{234}\text{Th}$  and  $^{238}\text{U}$  activities in deep waters which are in equilibrium within the reported 5% precision (BUESSELER *et al.*, 1992). The data quality for  $^{234}\text{Th}$  from leg 3 is comparable to that obtained in previous studies using the more labor intensive beta-counting techniques (SANTSCHI *et al.*, 1979, COALE and BRULAND, 1985).

### *Other data*

Sediment trap samples were collected from a free floating trap array of the VERTEX design (KNAUER *et al.*, 1979). Seven depths were sampled in the upper 2000 m, here we

report data from the shallowest traps at 150 and 300 m only. All traps were poisoned with a weak formalin brine solution. Total mass flux and organic carbon and nitrogen samples were collected from duplicate trap sampling tubes which were hand picked in an attempt to remove the zooplankton swimmers. Swimmers were found to represent 15–50% of the total sample weight from the 150 and 300 m traps, and consisted primarily of copepods (J. H. MARTIN, personal communication).

Material from a separate set of sampling tubes, not picked for swimmers, was analysed for  $^{234}\text{Th}$ . Samples (5–100 mg dry weight) were collected by filtering the entire contents of one or two trap tubes through 47 mm diameter filters. This could lead to a positive bias for the trap  $^{234}\text{Th}$  fluxes; but it is expected to be small because the specific activity of  $^{234}\text{Th}$  has been found to be 1–3 orders of magnitude lower in swimmers than in other trap material (COALE, 1990). The entire trap sample and filter were gamma counted using a high-purity germanium well detector.  $^{234}\text{Th}$  standards were made from varying quantities of sediment trap material (to determine geometry and self absorption effects) spiked with a  $^{238}\text{U}$  solution of known activity (BUESSELER *et al.*, 1992).

Particulate organic carbon and nitrogen (POC and PON) were determined on subsamples from 30-l Niskin or Go-Flo bottles which were filtered through glass fiber filters (precombusted 47 mm GF/F filters). Average POC and PON values corresponding to the particulate  $^{234}\text{Th}$  data are reported here for casts either just prior to or just after the *in situ* pump casts. The POC, PON and chlorophyll data were taken from SLAGLE and HEIMERDINGER (1991), and primary productivity data were provided by KNUDSON *et al.* (1989) and MARTIN *et al.* (1990).

## RESULTS

### $^{234}\text{Th}$

Dissolved and particulate  $^{234}\text{Th}$  results are given in Table 1, decay corrected to the mid-point of the sampling time. The surface water results (Fig. 1) show that at the start of the bloom, total  $^{234}\text{Th}$  ( $2.31 \text{ dpm l}^{-1}$ ) was only slightly lower than  $^{238}\text{U}$  ( $2.47 \text{ dpm l}^{-1}$ ). This indicates a slow rate of  $^{234}\text{Th}$  removal. By the beginning of May, other JGOFS investigators noticed a decrease in nutrient levels (nitrate dropped from 6 to less than  $5 \mu\text{mole l}^{-1}$ ) as the mixed layer shoaled and the major bloom activity was initiated. Our  $^{234}\text{Th}$  data followed a pattern similar to the nutrients, with an increase in the particulate concentrations as thorium was adsorbed onto newly formed particle surfaces. At the same time we saw a decrease in total  $^{234}\text{Th}$ , as thorium was removed from surface waters. The gap in the data (8–18 May) reflects the time when the ship was in port. When the site was reoccupied, total  $^{234}\text{Th}$  levels had dropped by 50%, indicating extensive removal as the bloom progressed. During the second half of May, surface water  $^{234}\text{Th}$  activities remained depleted, with some variability which may be attributable to mixing as well as continued scavenging. For instance, the storm which occurred around 20 May appears to have increased surface  $^{234}\text{Th}$  levels (and nutrients) via the upwelling of deeper waters (where  $^{234}\text{Th}$  levels are higher) into the mixed layer (see Discussion).

At the start and end of each occupation of the site, a shallow (0–300 m) profile for dissolved and particulate  $^{234}\text{Th}$  was obtained (Table 1 and Fig. 2). In late April, the mixed layer depth was greater than 100 m, and nitrate concentrations ( $\sim 6 \mu\text{mole l}^{-1}$ ) showed little surface depletion (Fig. 2a). Chlorophyll *a* (Chl *a*) concentrations were also low and

Table 1 Data from NABE for  $^{234}\text{Th}$  in the upper water column Values in parentheses are  $\pm$  errors

Date (dd/mm/1989)	Lat (°N)	Long (°W)	Depth (m)	Dissolved $^{234}\text{Th}$ (dpm l <sup>-1</sup> )	Part $^{234}\text{Th}$ (dpm l <sup>-1</sup> )	Total $^{234}\text{Th}$ (dpm l <sup>-1</sup> )	Part / Total (%)
24/04/	47 05 4	19 55 1	1	2 03 (0 21)	0 28 (0 03)	2 31 (0 21)	12
			50	1 82 (0 25)	0 46 (0 05)	2 28 (0 25)	20
			75	2 12 (0 22)	0 38 (0 04)	2 49 (0 23)	15
			100	2 34 (0 32)	0 11 (0 03)	2 45 (0 32)	5
			200	2 28 (0 31)	0 15 (0 02)	2 43 (0 31)	6
			300	2 48 (0 26)	0 13 (0 01)	2 61 (0 26)	5
28/04/	46 40 8	19 32 8	1	1 84 (0 09)	0 46 (0 05)	2 30 (0 11)	20
02/05/	46 36 1	20 14 2	1	1 71 (0 18)	0 38 (0 04)	2 09 (0 18)	18
05/05/	46 41 2	20 10 0	1	1 54 (0 16)	0 59 (0 06)	2 14 (0 17)	28
			25	1 18 (0 14)	0 75 (0 08)	1 93 (0 16)	39
			50	1 55 (0 16)	0 69 (0 07)	2 24 (0 17)	31
			75	2 16 (0 29)	0 25 (0 03)	2 41 (0 29)	11
			100	1 87 (0 20)	0 18 (0 02)	2 05 (0 20)	9
			200	2 49 (0 14)	0 03 (0 01)	2 52 (0 14)	1
			300	2 34 (0 32)	0 13 (0 02)	2 46 (0 32)	5
08/05/	46 26 7	19 07 1	1	1 27 (0 17)	0 60 (0 06)	1 87 (0 19)	32
18/05/	46 29 5	17 43 0	1	0 90 (0 05)	0 15 (0 01)	1 05 (0 05)	15
19/05/	46 29 7	17 49 5	1	0 33 (0 02)	0 29 (0 01)	0 62 (0 03)	47
			5	0 65 (0 05)	0 31 (0 03)	0 96 (0 06)	32
			20	0 95 (0 10)	0 33 (0 04)	1 28 (0 11)	26
			35	1 45 (0 15)	0 50 (0 05)	1 95 (0 16)	26
			50	1 66 (0 17)	0 46 (0 05)	2 12 (0 18)	22
			75	1 99 (0 14)	0 25 (0 03)	2 24 (0 14)	11
			150	2 12 (0 12)	0 19 (0 02)	2 30 (0 12)	8
			200	1 94 (0 10)	0 12 (0 02)	2 06 (0 10)	6
			300	2 00 (0 10)	0 12 (0 02)	2 13 (0 10)	6
22/05/	46 21 8	17 55 8	1	1 03 (0 05)	0 17 (0 01)	1 21 (0 05)	14
24/05/	46 20 3	17 56 0	1	0 36 (0 02)	0 28 (0 01)	0 64 (0 02)	44
26/05/	46 17 5	17 58 0	1	0 63 (0 04)	0 30 (0 02)	0 93 (0 04)	32
28/05/	46 19 5	17 50 4	1	0 81 (0 04)	0 38 (0 02)	1 19 (0 05)	32
30/05/	46 22 3	17 45 4	1	0 82 (0 04)	0 36 (0 02)	1 18 (0 05)	30
			20	0 96 (0 05)	0 49 (0 06)	1 45 (0 08)	34
			35	0 90 (0 05)	0 31 (0 04)	1 21 (0 06)	25
			50	1 19 (0 06)	0 21 (0 03)	1 40 (0 07)	15
			75	2 01 (0 11)	0 17 (0 02)	2 18 (0 11)	8
			100	1 91 (0 10)	0 12 (0 00)	2 03 (0 10)	6
			150	2 20 (0 12)	0 09 (0 00)	2 28 (0 12)	4
			200	2 18 (0 11)	0 09 (0 00)	2 27 (0 11)	4
300	2 30 (0 12)	0 07 (0 00)	2 38 (0 12)	3			
31/05/	46 22 3	17 45 4	1	0 35 (0 02)	0 32 (0 02)	0 67 (0 03)	48

Part = particulate

All data decay corrected to the time of sampling

The reported uncertainty includes errors due to blanks, counting statistics (one sigma), standardization and for dissolved  $^{234}\text{Th}$ , the MnO<sub>2</sub> adsorber sampling efficiency (see text and BUESSELER *et al*, 1992)

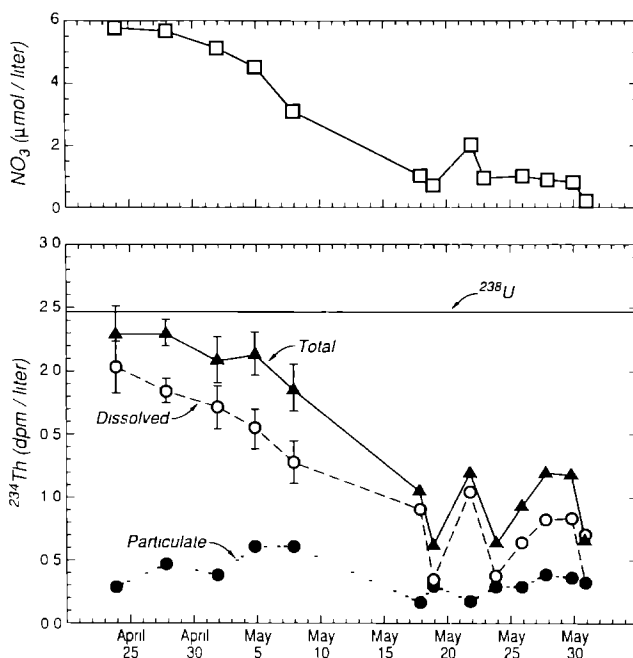


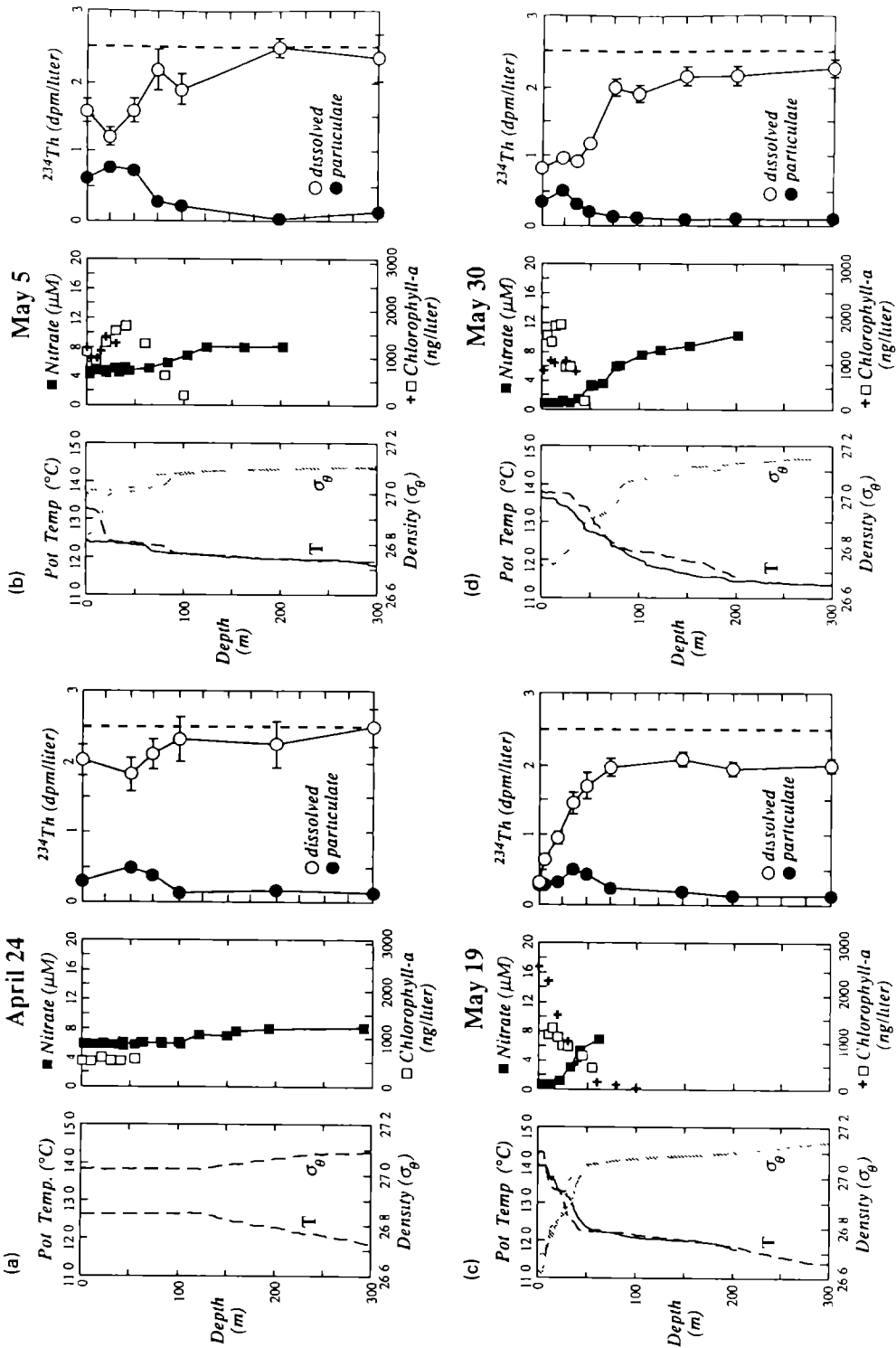
Fig 1 Time-series of nitrate (open squares—upper graph) plus dissolved (open circles), particulate (filled circles), and total  $^{234}\text{Th}$  (filled triangles) in surface water at  $47^{\circ}\text{N}$ ,  $20^{\circ}\text{W}$  study site. Horizontal line at  $2.47\text{ dpm l}^{-1}$  represents  $^{238}\text{U}$  activity predicted from CHEN *et al.* (1986) ( $^{238}\text{U} (\text{dpm l}^{-1}) = 0.0686 \times \text{salinity (psu)}$ ). Nitrate data taken from SLAGLE and HEIMERDINGER (1991).

uniform in the six samples collected in the upper 50 m ( $500\text{--}600\text{ ng l}^{-1}$ , Fig. 2a). This time period might be considered “pre-bloom” with respect to particle scavenging (see Discussion), but an apparent decrease in nitrate had occurred since an earlier occupation on 3 April, when mixed-layer nitrate levels of  $\approx 9.5\text{ }\mu\text{mole l}^{-1}$  were found (HONJO *et al.*, 1989). As was evident in the surface water data, the profile data showed only minor evidence of  $^{234}\text{Th}$  removal on 24 April. However, the particulate  $^{234}\text{Th}$  profile did show enhanced activities in the upper 100 m at that time.

By 5 May (Fig. 2b), stratification had developed (15–20 m mixed layer) and surface nitrate concentrations had dropped slightly to  $4.5\text{ }\mu\text{mole l}^{-1}$ . Pigments had increased substantially, with a subsurface Chl *a* maximum of  $1500\text{ ng l}^{-1}$  found at 30–50 m. Total  $^{234}\text{Th}$  activities were lower than equilibrium in the upper water column with a slight minimum at 25 m ( $1.9\text{ dpm l}^{-1}$ ), where a broad peak in particulate  $^{234}\text{Th}$  was also centered.

In mid-May (Fig. 2c), the depth of the mixed layer had not changed substantially, but continued warming of the surface waters and a strong decrease in surface nitrate levels ( $\sim 1\text{ }\mu\text{mole l}^{-1}$ ) were apparent. Chlorophyll *a* concentrations as high as  $2500\text{ ng l}^{-1}$  were found in the surface waters. Total  $^{234}\text{Th}$  activities in the surface waters were at their lowest at that time, indicating that substantial removal of  $^{234}\text{Th}$  had occurred. The disequilibrium between total  $^{234}\text{Th}$  and  $^{238}\text{U}$  now extended throughout the upper 300 m.

While  $^{234}\text{Th}$  was most strongly depleted in surface waters on 19 May, the greatest integrated  $^{234}\text{Th}$ -deficiencies were found on 30 May (Fig. 2d). Low levels of nitrate were



still detectable in surface waters ( $\sim 1 \mu\text{mole l}^{-1}$ ) and Chl *a* levels above  $1500 \text{ ng l}^{-1}$  were found in the upper 25 m.

Between 23 April and 1 June, three floating trap deployments were made at the NABE site. The  $^{234}\text{Th}$  profiles were taken at roughly the same time as the traps were launched ( $\pm 1$  day), thus the traps collected material over the same time periods as were considered in the  $^{234}\text{Th}$  scavenging model. The sediment trap fluxes were decay-corrected to the mid-point of the trap deployment. The sediment traps showed generally higher  $^{234}\text{Th}$  fluxes, total mass fluxes, and organic carbon and nitrogen fluxes in the 150 m trap relative to the 300 m trap (Table 2). Total trap mass and  $^{234}\text{Th}$  fluxes varied little during the course of the bloom. The organic carbon and nitrogen fluxes ranged from 7 to  $13 \text{ mmole C m}^{-2} \text{ day}^{-1}$  and from 0.7 to  $2.1 \text{ mmole N m}^{-2} \text{ day}^{-1}$ , respectively.

## DISCUSSION

### $^{234}\text{Th}$ scavenging models

Because of the conservative nature of uranium in the ocean, any deficiency of  $^{234}\text{Th}$  relative to  $^{238}\text{U}$  can always be attributed to the removal of Th, which is assumed to occur by scavenging and particle transport. A measurable disequilibrium ( $^{234}\text{Th}/^{238}\text{U}$  activity ratio  $< 1$ ) implies significant removal over a period that is shorter than a few times the  $^{234}\text{Th}$  half-life (24.1 days).

COALE and BRULAND (1985, 1987) used the observed distribution of dissolved and particulate  $^{234}\text{Th}$  and an irreversible scavenging model to estimate rates of Th uptake onto suspended particles and Th removal via sinking particles. These rates were calculated from the following two equations:

$$\frac{\partial A_{\text{Th}}^{\text{d}}}{\partial t} = A_{\text{U}} * \lambda - A_{\text{Th}}^{\text{d}} * \lambda - J_{\text{Th}} \quad (1)$$

and

$$\frac{\partial A_{\text{Th}}^{\text{p}}}{\partial t} = J_{\text{Th}} - A_{\text{Th}}^{\text{p}} * \lambda - P_{\text{Th}}, \quad (2)$$

where  $A_{\text{U}}$  = activity of  $^{238}\text{U}$ ,  $A_{\text{Th}}^{\text{d}}$  = activity of dissolved  $^{234}\text{Th}$ ,  $A_{\text{Th}}^{\text{p}}$  = activity of particulate  $^{234}\text{Th}$ ,  $\lambda$  =  $^{234}\text{Th}$  decay constant,  $J_{\text{Th}}$  = rate of uptake of dissolved  $^{234}\text{Th}$  onto particles, and  $P_{\text{Th}}$  = rate of loss of particulate  $^{234}\text{Th}$ . These equations neglect advection and diffusion, both of which are typically much smaller than the production and decay terms.

In most previous studies (KAUFMAN *et al.*, 1981, COALE and BRULAND, 1985, 1987,

Fig. 2. Vertical profiles (0–300 m) of  $^{234}\text{Th}$  and other data from four occupations of the 47°N site. Dashed vertical line represents expected  $^{238}\text{U}$  activity (CHEN *et al.*, 1986). Temperature, potential density, Chl *a*, and nitrate data are from SLAGLE and HEIMERDINGER (1991). Data correspond to the following NABE R/V *ATLANTIS II* stations and casts (sta–cast): (a) 24 April CTD 10–2,  $\text{NO}_3$  10–1, 10–3, 10–8, Chl *a* 10–1; (b) 5 May CTD 20–4 (solid), 20–6 (dashed),  $\text{NO}_3$  20–2, 20–6, Chl *a* 20–2 (crosses), 20–6 (squares); (c) 19 May CTD 26–4 (solid), 27–1 (dashed),  $\text{NO}_3$  26–2, Chl *a* 26–2 (crosses), 27–2 (squares); (d) 30 May CTD 37–3 (solid), 37–8 (dashed),  $\text{NO}_3$  37–3, 37–8, Chl *a* 37–3 (crosses), 38–1 (squares).

Table 2 Sediment trap data

Dates (dd/mm/1989)	Depth (m)	Tot flux ( $\text{mg m}^{-2} \text{day}^{-1}$ )	Org C flux ( $\text{mmol m}^{-2} \text{day}^{-1}$ )	N flux ( $\text{mmol m}^{-2} \text{day}^{-1}$ )	C/N ( $\text{mol mol}^{-1}$ )	$^{234}\text{Th}$ flux ( $\text{dpm m}^{-2} \text{day}^{-1}$ )	$^{234}\text{Th}$ ( $\text{dpm g}^{-1} \text{dry wt}$ )
24/4/-6/5/	150	670	7.2	1.3	5.54	1867	2040
	300	490	3.1	0.54	5.74	1279	2360
7/5/-20/5/	150	774	12.7	2.1	6.05	2145	1230
	300	435	5.4	0.80	6.75	1485	1060
22/5/-1/6/	150	545	11.6	2.00	5.80	1571	1120
	300	417	6.0	0.80	7.50	1498	1420

Total mass, organic C and N flux data from swimmer picked traps (J H MARTIN, personal communication)

$^{234}\text{Th}$  flux and specific activity data from unpicked traps (see text)

$^{234}\text{Th}$  flux and activity data are decay corrected to mid-point of trap deployment (see Appendix)



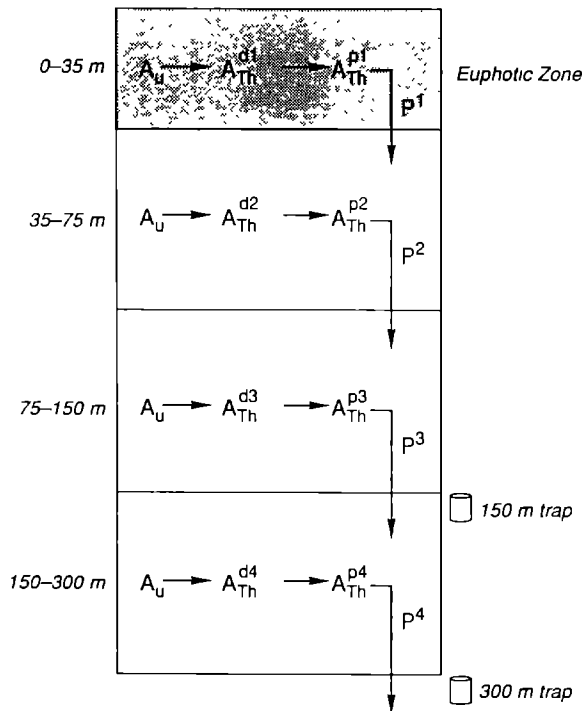


Fig 3 Schematic of  $^{234}\text{Th}$  model. See equations (3)–(7) in text for definitions of the terms

BRULAND and COALE, 1986), time-series data were not collected, and it was necessary to assume steady state ( $\partial A/\partial t = 0$  in (1) and (2)). From our data during the bloom, it is clear that both the dissolved and particulate  $^{234}\text{Th}$  activities do vary dramatically, and the assumption of steady state in the present case would not be valid ( $\partial A/\partial t \neq 0$ ). We therefore apply a non-steady state (NSS) form of the  $^{234}\text{Th}$  scavenging model to the NABE.

In the NSS model (Fig 3), the upper 300 m of the water column is divided into four layers, representing the euphotic zone (0–35 m—the 1% light level was found at 50–60 m in April and shallowed to  $\leq 35$  m by early May—KNUDSON *et al.*, 1989), sub-euphotic layer (35–75 m), and two deeper layers (75–150 m, 150–300 m). In contrast to some previous models, we include an additional source term for each sub-surface layer,  $P_{Th}^{i-1}$ , equal to the particulate  $^{234}\text{Th}$  flux from the layer above (Fig 3). For each layer,  $i$ , the NSS model equations are

$$\left. \frac{\partial A_{Th}^d}{\partial t} \right|^i = [A_U * \lambda]^i - [A_{Th}^d * \lambda]^i - J_{Th}^i \quad (3)$$

for dissolved  $^{234}\text{Th}$ ,

$$\left. \frac{\partial A_{Th}^p}{\partial t} \right|^i = J_{Th}^i + P_{Th}^{i-1} - [A_{Th}^p * \lambda]^i - P_{Th}^i \quad (4)$$

for particulate  $^{234}\text{Th}$ , and

$$\frac{\partial A_{\text{Th}}^{\text{tot}}}{\partial t} \Big|' = [A_{\text{U}} * \lambda]' - [A_{\text{Th}}^{\text{tot}} * \lambda]' + P_{\text{Th}}^{\prime-1} - P'_{\text{Th}} \quad (5)$$

for total  $^{234}\text{Th}$  ( $A_{\text{Th}}^{\text{tot}}$ ). In these equations,  $J$  represents the net of all forward and reverse exchange reactions, and  $P_{\text{Th}}^{\prime-1}$  is zero for the surface layer (Fig. 3). Given that the time interval is short (11–14 days) between  $^{234}\text{Th}$  profiles relative to the half-life, we have used a linear approximation to the solutions of equations (3) and (5) to determine  $J$  and  $P$  (see Appendix A for exact solutions). This approximation introduces an error of only  $\approx 1\%$  to the calculated fluxes. The equations used are

$$J'_{\text{Th}} = \lambda \left[ A_{\text{U}} - \frac{(A_{\text{Th}-1}^{\text{d}} + A_{\text{Th}-2}^{\text{d}})}{2} \right]' - \left[ \frac{(A_{\text{Th}-2}^{\text{d}} - A_{\text{Th}-1}^{\text{d}})}{t_2 - t_1} \right]' \quad (6)$$

and

$$P'_{\text{Th}} = P_{\text{Th}}^{\prime-1} + \lambda \left[ A_{\text{U}} - \frac{(A_{\text{Th}-1}^{\text{tot}} + A_{\text{Th}-2}^{\text{tot}})}{2} \right]' - \left[ \frac{(A_{\text{Th}-2}^{\text{tot}} - A_{\text{Th}-1}^{\text{tot}})}{t_2 - t_1} \right]', \quad (7)$$

where  $t_1$  and  $t_2$  represent the beginning and end of the time interval and  $A_{\text{Th}-1}$  and  $A_{\text{Th}-2}$  are the measured  $^{234}\text{Th}$  activities at  $t_1$  and  $t_2$ .  $A_{\text{Th}}$  values were obtained for each layer via trapezoidal integration of the activity profiles in Table 1.  $^{238}\text{U}$  activities were obtained from salinity ( $^{238}\text{U}$  (dpm  $\text{l}^{-1}$ ) = 0.0686  $\times$  salinity, CHEN *et al.*, 1986). The calculated  $^{234}\text{Th}$  fluxes are reported in Table 3.

In the calculation of  $P$  from equation (7), the change in particulate  $^{234}\text{Th}$  with time is most significant early in the bloom, when  $\partial A_{\text{Th}}^{\text{p}}/\partial t$  was large and positive (Fig. 4). Had we treated  $^{234}\text{Th}$  as being in steady state ( $\partial A/\partial t = 0$ ), the calculated particle fluxes would have been incorrect. For example the particle flux,  $P$ , at 35 m during 24 April to 5 May would be four times smaller had we assumed steady state. In general, when  $^{234}\text{Th}$  inventory is decreasing ( $\partial A/\partial t < 0$ —at the onset of more intense scavenging) steady state removal times calculated for  $^{234}\text{Th}$  will be too long, and with increasing  $^{234}\text{Th}$  inventories ( $\partial A/\partial t > 0$ —for example during post-bloom conditions) steady state removal time estimates for  $^{234}\text{Th}$  will be too short.

Few previous studies of oceanic  $^{234}\text{Th}$  scavenging have included time-series data for comparison to the NABE data set. The most complete time-series analyses are those of TANAKA *et al.* (1983), who compared nine profiles of total  $^{234}\text{Th}$  measured during a 1 year period in Funka Bay, Japan. They found large variations in the total  $^{234}\text{Th}$  activities which they proposed were related to biological activity in the surface waters, since the minimum in  $^{234}\text{Th}$  inventory coincided with the early spring bloom. They calculated that  $^{234}\text{Th}$  residence times could differ by up to a factor of four between steady state and NSS models. BRULAND and COALE (1986) found that the activities of dissolved  $^{234}\text{Th}$  in the central Pacific gyre increased by 25–30% between March and September, and this affected their steady state residence time of dissolved  $^{234}\text{Th}$  by a factor of 3. KU and KUSAKABE (1990) show mathematically that a NSS model must be considered for  $^{234}\text{Th}$  when the residence time for total  $^{234}\text{Th}$  is greater than 10–20 days, given a scenario in which half of the  $^{234}\text{Th}$  has been scavenged during a bloom. Significant discordancy can exist between residence time estimates made using both  $^{234}\text{Th}$  and the longer lived thorium tracer  $^{228}\text{Th}$  ( $t_{1/2} = 1.9$  y; KAUFMAN *et al.*, 1981, SANTSCHI *et al.*, 1979) if a steady state model is used and the system has not reestablished equilibrium conditions.

Table 3 Model flux results and carbon and nitrogen flux calculations Values in parentheses are best estimates using 150 m trap ratios extrapolated to shallower depths

Dates (dd/mm/1989)	Depth (m)	$P \pm \text{error}^*$ ( $\text{dpm m}^{-3} \text{ day}^{-1}$ )	$J \pm \text{error}^*$ ( $\text{dpm m}^{-3} \text{ day}^{-1}$ )	(Filter) POC/Th $^{\ddagger}$ ( $\mu\text{mol dpm}^{-1}$ )	(Trap) Org C/Th $^{\ddagger}$ ( $\mu\text{mol dpm}^{-1}$ )	(High) C-flux $\S$ ( $\text{mmol m}^{-2} \text{ day}^{-1}$ )	(Low) C-flux $\ $ ( $\text{mmol m}^{-2} \text{ day}^{-1}$ )	(Filter) PON/Th $^{\ddagger}$ ( $\mu\text{mol dpm}^{-1}$ )	(Trap) Org N/Th $^{\ddagger}$ ( $\mu\text{mol dpm}^{-1}$ )	(High) N-flux $\S$ ( $\text{mmol m}^{-2} \text{ day}^{-1}$ )	(Low) N-flux $\ $ ( $\text{mmol m}^{-2} \text{ day}^{-1}$ )
24/4/-5/5/	35	1280 $\pm$ 790	-2990 $\pm$ 760	14.2	(3.9)	18.2	(5.0)	2.2	(0.7)	2.8	(0.9)
	75	1720 $\pm$ 900	-1470 $\pm$ 870	20.5	(3.9)	35.3	(6.7)	3.2	(0.7)	5.5	(1.2)
	150	4560 $\pm$ 2320	-3500 $\pm$ 2300	15.0	3.9	68.4	17.6	2.3	0.7	10.5	3.2
	300	4260 $\pm$ 3770	1000 $\pm$ 3800	10.6	2.4	45.2	10.3	1.7	0.4	7.2	1.8
5/5/-19/5/	35	2610 $\pm$ 330	-2300 $\pm$ 300	15.7	(5.9)	41.0	(15.4)	2.5	(1.0)	6.5	(2.6)
	75	3350 $\pm$ 510	-850 $\pm$ 480	23.0	(5.9)	77.1	(19.8)	3.5	(1.0)	11.7	(3.4)
	150	3090 $\pm$ 1100	-300 $\pm$ 1090	11.8	5.9	36.5	18.3	1.8	1.0	5.6	3.0
	300	7750 $\pm$ 1710	-5800 $\pm$ 1700	8.0	3.6	62.0	28.2	1.4	0.5	10.9	4.2
19/5/-30/5/	35	1050 $\pm$ 240	-1610 $\pm$ 200	22.5	(7.4)	23.6	(7.7)	3.3	(1.3)	3.5	(1.4)
	75	3600 $\pm$ 420	-2230 $\pm$ 400	14.3	(7.4)	51.5	(26.6)	2.1	(1.3)	7.6	(4.7)
	150	5060 $\pm$ 780	-1140 $\pm$ 770	8.9	7.4	45.0	37.3	1.4	1.3	7.1	6.4
	300	3580 $\pm$ 1350	1660 $\pm$ 1340	7.9	4.0	28.3	14.4	1.4	0.5	5.0	1.9

\*  $P$  and  $J$  represent the net flux of particulate and dissolved  $^{234}\text{Th}$ , respectively, as defined in equations (3) and (4). Errors are propagated from terms in equations (6) and (7).

$^{\ddagger}$  C/Th and N/Th are from POC, PON and particulate  $^{234}\text{Th}$  data averaged at the depth of interest and collected either 1 day before or after the  $^{234}\text{Th}$  east

$\S$  The organic C/ $^{234}\text{Th}$  and N/ $^{234}\text{Th}$  ratios at 150 m are taken from the floating trap data in Table 2

$\|$  High flux estimate is from particle flux  $P$  and the POC/ $^{234}\text{Th}$  or PON/ $^{234}\text{Th}$  ratios

$\|$  Low flux estimate is from particle flux  $P$  and the trap organic C/ $^{234}\text{Th}$  or N/ $^{234}\text{Th}$  ratio

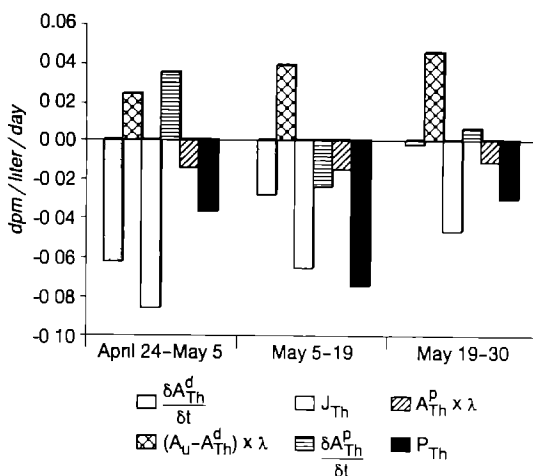


Fig 4 Model supply and removal terms from equations (6) and (7) plotted for the 0–35 m layer during three time intervals. Values above zero represent net gains of  $^{234}\text{Th}$ , and values below zero represent net losses of  $^{234}\text{Th}$ .

The consequences of assuming steady state in  $^{234}\text{Th}$  scavenging models will be large or small depending upon the extent of  $^{234}\text{Th}$   $^{238}\text{U}$  disequilibria and the range of temporal variability. The need to model the North Atlantic spring bloom as a non-steady state process may not be surprising given the strong seasonal variation seen here in surface ocean productivity (BROWN *et al.*, 1985, ESAIAS *et al.*, 1986). If blooms such as this are globally important for the export of carbon and associated nutrients, it would be necessary to sample the bloom period in a time-series fashion and use a non-steady state approach to accurately estimate export fluxes.

#### $^{234}\text{Th}$ fluxes

The dissolved and particulate fluxes of  $^{234}\text{Th}$  estimated from the NSS model show considerable variability during the NABE (Fig 5). The values for  $J$  and  $P$  found here for the euphotic zone range from 1600 to 3000 and 1000 to 2600  $\text{dpm m}^{-2} \text{day}^{-1}$ , respectively. These values are similar to previous estimates for productive coastal regions (COALE and BRULAND, 1985). The NABE particulate  $^{234}\text{Th}$  fluxes are also similar to those reported along  $160^\circ\text{W}$  (BRULAND and COALE, 1986) and across the Galapagos Front (MURRAY *et al.*, 1989) in the equatorial Pacific. Lower estimates of upper ocean  $^{234}\text{Th}$  export are found in the oligotrophic gyres (BRULAND and COALE, 1986; COALE and BRULAND, 1987).

The pattern of export fluxes estimated for the NABE appears to be related to the evolution of the spring bloom. Consider the euphotic zone first. The  $^{234}\text{Th}$  export flux,  $P$ , increases from 1300 to 2600  $\text{dpm m}^{-2} \text{day}^{-1}$  between late April and the first half of May (Fig. 5 and Table 3). Subsequently, it decreases to 1000  $\text{dpm m}^{-2} \text{day}^{-1}$  by the second half of May. The model  $^{234}\text{Th}$  flux at 75 m is similar to the flux at 35 m during the first two time intervals, indicating little net change in export from the 35–75 m layer. During the latter half of May, in contrast, the flux at 75 m for  $^{234}\text{Th}$  is much larger than at 35 m, indicating a net increase in the 35–75 m layer of 2600  $\text{dpm m}^{-2} \text{day}^{-1}$ . This increase is of the same order as the maximum export flux found at 35 m during the first half of May. These results

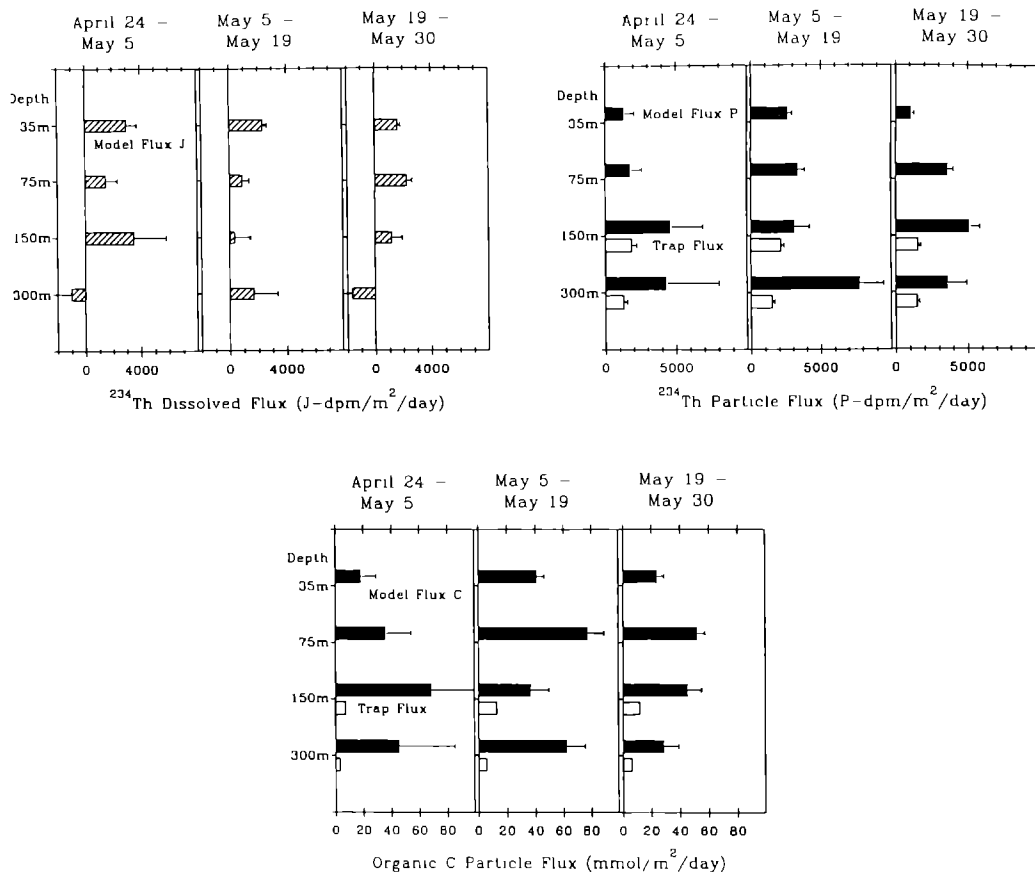


Fig 5 Model-derived fluxes during three time intervals for dissolved  $^{234}\text{Th}$ , particulate  $^{234}\text{Th}$  and particulate organic carbon (high estimate for C in Table 3) The model particulate fluxes (solid bars) at 150 and 300 m are compared to the measured trap fluxes (open bars) at the same depths and time intervals. Error estimates are also plotted. See text for details.

suggest that as the bloom progresses, a two-layered system is established, with more of the export originating below the mixed layer in the later stages of the bloom. Similar stratification has been found in oligotrophic waters (GIESKES and KRAAY, 1986, SMALL *et al.*, 1987, COALE and BRULAND, 1987).

The deeper export estimates can be compared directly to the floating sediment trap results at 150 and 300 m. It should be noted that we also used a linear approximation in correcting the trap flux for decay back to the mid-point of the deployment. A more exact treatment is given in the Appendix. Because the trap deployments were short in duration relative to the half-life of  $^{234}\text{Th}$ , the error introduced by the approximation is less than 1%.

The errors in the model fluxes are large for late April (Fig. 5), due to the poorer  $^{234}\text{Th}$  data quality on leg 2 and the fact that the deep  $^{234}\text{Th}$  values were close to equilibrium with  $^{238}\text{U}$  (Fig. 2). The quality of the deep water data is better in mid- and late May, and it is here that the comparison between the model and measured  $^{234}\text{Th}$  trap fluxes can best be made. The NSS model fluxes are always greater than those measured with the traps in

May; however, in mid-May at 150 m the two estimates overlap within errors. A positive or negative collection bias of a factor of 2–3 between upper ocean  $^{234}\text{Th}$  trap fluxes and those calculated from  $^{234}\text{Th}$  water column distributions are in fact quite common (BUESSELER, 1992). Overall, the trap fluxes show less temporal variability during the course of the bloom than is estimated by the NSS model. These differences in flux estimates between the traps and the NSS model suggest either problems with using the floating trap array to collect particles fluxes from the upper 300 m or deficiencies in the NSS model.

The two major assumptions which are used here to estimate the  $^{234}\text{Th}$  fluxes with the NSS model are. (1) the four vertical  $^{234}\text{Th}$  profiles are representative of changes during the course of the bloom in scavenging at the NABE site (i.e. spatial variability in export is small) and (2) the advective and diffusive fluxes of  $^{234}\text{Th}$  between the model layers are negligible.

The first assumption implies that we always sampled the same water mass, or at least that spatial variability in scavenging is small. Studies by ROBINSON *et al.* (in press) have identified three major eddies in the region of  $46^{\circ}$ – $51^{\circ}\text{N}$  and  $16^{\circ}$ – $22^{\circ}\text{W}$  during the NABE. Our sampling was conducted within  $46.10^{\circ}$ – $47.10^{\circ}\text{N}$  and  $17.40^{\circ}$ – $20.20^{\circ}\text{W}$  or at the edge of a small eddy (roughly 150 km diameter). This eddy was identified by altimeter data and by XBT and CTD surveys. Within the small eddy, a mean cyclonic surface current of  $20\text{ cm s}^{-1}$  was found. Water sampled at a fixed point therefore will have travelled a lateral distance of 150–200 km between our sampling dates. As a first approximation we must assume that spatial variability in surface particle fluxes within the eddy was small. Small scale patchiness in temperature and ocean color (i.e. chlorophyll levels) was seen within the eddies (ROBINSON *et al.*, in press), however, the main features in the data at the start of the bloom are the systematic decreases in surface  $^{234}\text{Th}$  along with  $\text{NO}_3$  (Fig. 1) and  $\text{pCO}_2$  (GOYET and BREWER, submitted a). This is consistent with the sampling of a single biological community and not the random sampling of different water masses with widely differing scavenging histories. The scatter in the surface water data in mid-May (Fig. 1) appears to be driven by storm activity and upwelling which occurred after our 19 May  $^{234}\text{Th}$  profile (see discussion on diffusive and advective terms).

The overall decrease in total  $^{234}\text{Th}$  which dominates the surface water time-series is also seen in integrated  $^{234}\text{Th}$  inventories in the upper 100 m. Below 100 m, one can also see a general decrease in  $^{234}\text{Th}$  inventories between late April/early May and the second half of May, consistent with continued scavenging at this site. The waters between 100 and 300 m do, however, show variations in T/S properties (SLAGLE and HEIMERDINGER, 1991) with a general trend of decreasing temperature and increasing density with time (Fig. 2). A change in deep-water properties might imply the sampling of different water masses; however, colder waters would tend to be  $^{234}\text{Th}$  enriched (i.e. deeper sources), and ignoring this source term in our NSS box model would result in an overall underestimation of the true  $^{234}\text{Th}$  fluxes. Unfortunately, we do not have both spatial and temporal  $^{234}\text{Th}$  data with which to address this issue more rigorously.

The floating sediment traps collect an average particle flux which has a horizontal length scale related to the kinetic energy field above the trap and the particle sinking speed. If the trap is a perfect collector, then using the analysis of SIEGEL *et al.* (1990) it can be estimated that a fixed trap at 150 m would collect sinking particles over a horizontal scale of 5–100 km (equation (11) in SIEGEL *et al.* (1990), with eddy kinetic energy =  $10$ – $100\text{ cm}^2\text{ s}^{-2}$  and particle sinking speeds of  $15$ – $150\text{ m day}^{-1}$ ). Depending upon the speed of the 150 m trap relative to the water at that depth (remember that the NABE floating traps extended down

to 2000 m), the horizontal averaging scale might be slightly less than this. The above calculations suggest that the  $^{234}\text{Th}$  model fluxes and the trap fluxes at 150 m should be considered as averages over horizontal scales of 10s to 100s of kilometers, i.e. over the same scale as the small eddy within which the majority of the NABE measurements were made

The second assumption in the NSS  $^{234}\text{Th}$  model is the absence of vertical advective and diffusive fluxes between the layers. With a vertical eddy diffusivity ( $K_z$ ) of  $10^{-4} \text{ m}^2 \text{ s}^{-1}$  and an average vertical advection velocity ( $w$ ) of  $2\text{--}10 \text{ m y}^{-1}$ , the calculated advective and diffusive  $^{234}\text{Th}$  flux ( $F = K_z * \partial\text{Th}/\partial z + w * \text{Th}$ ) between the upper two layers in mid-April is only 5–10% of the observed particle flux ( $\partial\text{Th}/\partial z = 20 \text{ dpm m}^{-4}$ ,  $\text{Th} = 2 \times 10^3 \text{ dpm m}^{-3}$ )

While we have shown that advection and diffusion can generally be neglected in the NSS model, short term intensification of mixing can occur. An example of increased mixing was the storm on 19–20 May. To a first approximation, if upwelling due to this event was confined to the 0–35 m layer, then there is no net effect on the NSS model. Significant entrainment of waters deeper than 35 m due to this storm is unlikely, given that the mixed layer depth (10–15 m) remained well within the upper 35 m throughout the second half of May. The observed surface water increases in  $^{234}\text{Th}$  (Fig. 1) can also be accounted for if upwelling is contained within the 0–35 m layer. As stated above, if deeper waters are a significant source of  $^{234}\text{Th}$ , then our model fluxes would tend to underestimate the true vertical fluxes

#### *New production estimates*

New production refers to the fraction of total primary production in the oceans which is supported by the input of nutrients to the euphotic zone. In the North Atlantic, nutrients are depleted during the spring and summer from stratified surface waters and renewed during winter mixing. Common methods to determine new production are: (a) bottle incubations with  $^{15}\text{NO}_3$  and  $^{15}\text{NH}_4$  to measure assimilation based upon new ( $\text{NO}_3$ ) or recycled ( $\text{NH}_4$ ) nitrogen sources (DUGDALE and GOERING, 1967), (b) direct measurements at the base of the euphotic zone of organic C or N export (assumed to balance new production) using sediment traps (EPPLEY and PETERSON, 1979; HARGRAVE, 1985, PACE *et al.*, 1987), and (c) calculations from seasonal changes in oxygen, nutrients and  $\text{CO}_2$  distributions (JENKINS, 1982, JENKINS and GOLDMAN, 1985). EPPLEY (1989) proposed a fourth method, which was to use the residence time of  $^{234}\text{Th}$  and the measured POC inventory to calculate rates of new production in carbon units. This assumes a similar particle residence time for  $^{234}\text{Th}$  and organic C which, as pointed out by MURRAY *et al.* (1989), is generally not the case.

In this study, we take a somewhat different approach than EPPLEY (1989) proposed for using  $^{234}\text{Th}$  to calculate new production rates. As discussed above, we can estimate  $^{234}\text{Th}$  particle fluxes out of the surface ocean from the measured  $^{234}\text{Th}$  distributions and the NSS model. Given the calculated  $^{234}\text{Th}$  export fluxes, it is possible to estimate carbon and nitrogen export if  $\text{POC}/^{234}\text{Th}$  or  $\text{PON}/^{234}\text{Th}$  ratios on sinking particle can be determined. It is an empirical approach that does not require the assumption of equal residence times for particulate C and Th.

In our analysis, the estimated export terms for organic C and N are limited primarily by how well one can constrain the  $\text{POC}/^{234}\text{Th}$  and  $\text{PON}/^{234}\text{Th}$  ratios of the sinking particle

pool. For export at the base of the euphotic zone (>95% of the production occurs here within the upper 35 m—KNUDSON *et al.*, 1989, MARTIN *et al.*, 1990) we have used two approaches to this problem. We propose that an upper limit of C and N export can be calculated using the model  $^{234}\text{Th}$  particle flux from the upper 35 m and the C/ $^{234}\text{Th}$  and N/ $^{234}\text{Th}$  ratios measured at 35 m from POC and PON data and particulate  $^{234}\text{Th}$  activities. We believe it is an upper limit estimate because, with the aggregation of small suspended particles into rapidly sinking ones, some C and N may be preferentially lost relative to Th. When the suspended particulate ratios are compared to the traps—this is possible at 150 and 300 m—then a C/ $^{234}\text{Th}$  and N/ $^{234}\text{Th}$  ratio difference of 20–80% is seen, with the sediment trap values always being lower (Table 3).

Since we did not obtain samples of sinking particles at the base of the euphotic zone directly, a lower limit on C and N export can be estimated by using the 35 m particle flux from the NSS model, and the measured C/ $^{234}\text{Th}$  and N/ $^{234}\text{Th}$  ratios from the shallowest floating trap at 150 m. We believe this is a lower limit estimate since some preferential remineralization of C and N relative to Th has likely occurred between 35 m and the first trap at 150 m. We see such a loss, for example, between the 150 and 300 m traps, where the deeper C/ $^{234}\text{Th}$  and N/ $^{234}\text{Th}$  ratios in the trap are consistently lower (Table 3).

Thus we do not rely on the absolute fluxes measured by the sediment traps, but we do assume that the traps collect a representative sample of the material that is sinking. Here we ignore a number of potential problems with shallow traps, such as: (a) a significant fraction, even a majority, of the organic material collected is often attributed to swimmers (i.e. a non-passive flux), which are extremely difficult to separate or even elucidate (LEE *et al.*, 1988, MICHAELS *et al.*, 1990), (b) in high shear environments, such as are more common in the upper ocean, traps may serve as selective particle filters, preferentially over or under sampling particles of different size classes (GARDNER, 1980a,b, BUTMAN *et al.*, 1986), thus possibly biasing composition as well as flux, (c) decomposition and dissolution of material may alter the composition (KNAUER *et al.*, 1984), and (d) the vertical migration of zooplankton can cause traps to underestimate export fluxes if the migrators feed above the trap and defecate below (ANGEL, 1989). All of these factors could alter the measured trap C/ $^{234}\text{Th}$  ratio from the true value needed to estimate export. Our study cannot resolve these issues, rather the trap ratio data are simply used as a second constraint on the model flux estimates.

The organic C and N flux estimates are summarized in Table 3 and plotted for organic C in Fig. 5. Not surprisingly, the C export flux from the upper 35 m peaks in the first half of May, similar to  $^{234}\text{Th}$ . A two-layered structure for export is also seen in the C and N fluxes, with increased export in the 35–75 m layer by mid-May. Since the C/ $^{234}\text{Th}$  and N/ $^{234}\text{Th}$  ratios decrease with depth (Table 3) the C and N fluxes drop off more sharply with depth than does the  $^{234}\text{Th}$  flux (Fig. 5). It is clear that neither the POC/ $^{234}\text{Th}$  or PON/ $^{234}\text{Th}$  ratios obtained from data collected at 35 m (i.e. base of euphotic zone) nor the trap derived organic C/ $^{234}\text{Th}$  or N/ $^{234}\text{Th}$  ratio from 150 m are an ideal estimate of these ratios in the true sinking flux. However, we are encouraged that by using these ratios as limits, we have constrained the organic C and N export flux on particles quite well.

In designing future studies employing  $^{234}\text{Th}$  to estimate export flux, it would be highly desirable if POC, PON and particulate  $^{234}\text{Th}$  are all measured on the same sample filter. Separate analysis of large particles collected by filtering through coarse mesh screen, should also be done to obtain POC/ $^{234}\text{Th}$  and PON/ $^{234}\text{Th}$  that should be more representative of sinking material than the particles collected on standard filters. In principle, this



would make it possible to obtain independent estimates of export flux that avoid the problems of sediment traps altogether.

From late April through May,  $\geq 95\%$  of the primary production occurred within the upper 35 m and production levels remained relatively constant (calculated from data in KNUDSON *et al.*, 1989 and MARTIN *et al.*, 1990). If we examine the ratio of particle export to total production (*f*-ratio), then we find the lowest *f*-ratios during the 24 April–5 May and 19–30 May periods (Table 4). During these intervals, 5–27% of the primary production is lost as a sinking particulate flux. The largest C export flux from the upper 35 m occurred during the 5–19 May interval, when *f*-ratios were 16–42%. A similar pattern is found for nitrogen export, with peak export occurring in the first half of May (Table 4). The calculations made here for the *f*-ratio use integrated primary productivity data from multiple depths, averaged over many determinations during periods of 10–14 days. Over short time scales, export fluxes and new production based upon nutrient uptake experiments need not balance.

The above outlined progression of C and N export is consistent with the overall plankton succession during the NABE. At the start of the bloom, a mixed coccolithophorid and diatom assemblage evolved into one dominated entirely by diatoms. Particle export peaked during this diatom-dominated phase. Following silicate depletion in mid-May, small flagellates were found to dominate the surface plankton community (VERITY *et al.*, 1990). Verity *et al.* suggest that the small protozoans (primarily ciliates) had sufficiently high grazing rates to consume the bulk of the primary production, thereby limiting particle export. The expected decrease in export can indeed be seen in the surface NSS model fluxes (Fig. 5).

#### *Comparison between estimated and observed losses of N and C*

Our estimates of export production during the NABE can be compared directly to the observed changes in total N inventory. In this analysis, total nitrogen is taken to include nitrate, nitrite and PON (ammonium is low in surface waters and DON is assumed constant). From N data collected on the same dates as  $^{234}\text{Th}$  (Fig. 2, SLAGLE and HEIMERDINGER, 1991), the N losses from the 0–35 m layer during the three sampled intervals were 1.4, 7.4 and 0.9 mmole  $\text{m}^{-2} \text{day}^{-1}$ . Taking into account the errors in the particle flux *P*, the estimated high and low N fluxes overlap with these observed losses (Table 3). Furthermore, this comparison suggests that the N fluxes early and late in the bloom are better estimated using the  $\text{N}/^{234}\text{Th}$  ratio from the trap (i.e. the lower N flux estimate). In contrast, during peak export in the first half of May, the higher flux based upon the  $\text{PON}/^{234}\text{Th}$  ratio is closest to the observed N loss. During higher flux periods, sinking particles would appear to more closely resemble the suspended particulate pool. During lower flux intervals, the sinking particles have apparently lost significant N relative to  $^{234}\text{Th}$  in comparison to the suspended particulates. Given that the particle fluxes balance the observed N loss, dissolved organic nitrogen (DON) does not need to play a large role to account for N export during the NABE, such as has been recently postulated for DOC (SUGIMURA and SUZUKI, 1988, TOGGWEILER, 1989).

The comparison between estimated and observed fluxes can also be made for carbon. The change in total  $\text{CO}_2$  from 25 April to 30 May yields a total loss of carbon from the upper 125 m which is of the order of 63 mmole  $\text{C m}^{-2} \text{day}^{-1}$  (GOYET and BREWER, submitted b). In a separate analysis, SUZUKI *et al.* (1991) suggest an organic C loss from

Table 4 Carbon and nitrogen fluxes, productivity and f-ratios from the euphotic zone (0–35 m)

Dates (dd/mm/1989)	Depth (m)	Org C flux* (mmol m <sup>-2</sup> day <sup>-1</sup> )	Productivity† (mmol C m <sup>-2</sup> day <sup>-1</sup> )	f-ratio‡	Org N flux§ (mmol m <sup>-2</sup> day <sup>-1</sup> )	Production   (mmol N m <sup>-2</sup> day <sup>-1</sup> )	f-ratio¶
24/4/-5/5/	35	5.0–18.2	91	0.05–0.20	0.9–2.8	13	0.07–0.22
5/5/-19/5/	35	15.4–41.0	98	0.16–0.42	2.6–6.5	14	0.19–0.46
19/4/-30/5/	35	7.8–23.6	87	0.09–0.27	1.4–3.5	12	0.12–0.29

\*Carbon flux estimates from NSS model and C/<sup>234</sup>Th ratios (Table 3). Lower limit calculated from 150 m trap C/<sup>234</sup>Th ratio and upper limit from POC/<sup>234</sup>Th ratios at 35 m (see text for details).

†Primary production averaged over upper 35 m during time intervals of interest. Data from KNUDSEN *et al.* (1989) and MARTIN *et al.* (1990).

‡f-ratio = C flux/C production.

§Nitrogen flux estimates from NSS model and N/<sup>234</sup>Th ratios (Table 3). Lower limit calculated from trap N/<sup>234</sup>Th ratio and upper limit from PON/<sup>234</sup>Th ratios at 35 m (see text for details).

||Primary production in nitrogen units from: C production × 1/7.

¶f-ratio = N flux/N production.

the upper 100 m of  $\sim 20\text{--}50 \text{ mmole C m}^{-2} \text{ day}^{-1}$  based upon the variation in total organic C between the spring and estimated winter values. Both of these estimates are significantly higher than the C fluxes obtained with the floating traps (Table 2), but are similar to the estimates derived from  $^{234}\text{Th}$  (Table 3)

### *Pre-bloom particle scavenging*

Upon our arrival at the NABE study site on 24 April,  $^{234}\text{Th}$  activities were close to equilibrium with  $^{238}\text{U}$ , indicating relatively little particle export prior to our first sampling. Using the 24 April  $^{234}\text{Th}$  data (Table 1) we estimate a pre-arrival surface particulate  $^{234}\text{Th}$  flux of  $5 \text{ dpm m}^{-3} \text{ day}^{-1}$  for  $^{234}\text{Th}$  (assuming  $\partial A/\partial t = 0$  since the initial rate of change is very small—Fig. 1). Using a N/ $^{234}\text{Th}$  ratio of  $1\text{--}2 \mu\text{mole dpm}^{-1}$  (Table 3), the estimated N loss via particle scavenging would have been of the order of  $5\text{--}10 \mu\text{mole N m}^{-3} \text{ day}^{-1}$ . From a surface layer of 50–100 m thickness, the integrated N loss would total  $0.25\text{--}1 \text{ mmole N m}^{-2} \text{ day}^{-1}$ . This is consistent with an  $f$ -ratio less than 0.1, and the observed productivity levels of  $10\text{--}15 \text{ mmole N m}^{-2} \text{ day}^{-1}$  in late April.

The  $^{234}\text{Th}$  data therefore suggest relatively minor N export prior to our arrival on 24 April, when nitrate concentrations of  $6 \mu\text{mole l}^{-1}$  were found in the mixed layer. These nitrate levels are much lower than those reported by HONJO *et al.* (1989) on 3 April at this site ( $\text{NO}_3 = 9.5 \mu\text{mole l}^{-1}$ ) and also lower than concentrations predicted by GLOVER and BREWER (1988) as the initial winter mixed layer value for this location ( $\text{NO}_3 = 12 \mu\text{mole l}^{-1}$ ). One explanation for the early drop in nitrate might be that early in the bloom, nitrate is lost to an unmeasured DON pool. We believe, however, that it is more likely that these apparently large “pre-bloom” nitrate losses are due to the advective transport of low nitrate waters to the study site prior to our arrival, rather than by particle export or conversions to DON. This is supported by an observed salinity change from 35.55 to 35.71 psu between 3 and 24 April, with waters only a few degrees south of  $47^\circ\text{N}$ ,  $20^\circ\text{W}$  having both the appropriate higher salinity and winter nitrate levels around  $6 \mu\text{mole l}^{-1}$ .

## SUMMARY AND CONCLUSIONS

We have used four profiles of dissolved and particulate  $^{234}\text{Th}$  obtained between 24 April and 30 May 1989 to quantify particle export of  $^{234}\text{Th}$ , organic C and N during the North Atlantic spring bloom. Our main conclusions are as follows:

(1) In late April, the uptake of dissolved  $^{234}\text{Th}$  onto suspended particles dominated the  $^{234}\text{Th}$  balance, and particle export was small. The dissolved  $^{234}\text{Th}$  uptake rates correlate with the depletion of inorganic N. Both total  $^{234}\text{Th}$  and nitrogen levels decrease in surface waters by the beginning of May.

(2) A non-steady state model was needed to estimate the particle flux out of the upper water column. The observed change in  $^{234}\text{Th}$  activity with time is often the largest term in the budget, illustrating the need for time-series measurements during the bloom.

(3) The highest estimated particle fluxes occurred during the first half of May. Using organic C/ $^{234}\text{Th}$  and N/ $^{234}\text{Th}$  ratios, C and N fluxes are estimated for the base of the euphotic zone (35 m), and at 75, 150 and 300 m. All of the flux estimates show the development of a two-layered stratification by mid- to late May, with a relatively small particle flux out of the 0–35 m layer and higher fluxes below (35–75 m).

(4) Our best estimate of export from the upper 35 m suggests that the lowest particle

losses relative to production occurred at the start and end of the bloom ( $f$ -ratios as low as 0.05–0.10). A peak in organic C and N export occurred during the 5–19 May time period, when  $f$ -ratios were as high as 0.4.

(5) The integrated loss of total N ( $\text{NO}_3 + \text{NO}_2 + \text{PON}$ ) averaged over the upper 35 m agrees with the fluxes estimated from the  $^{234}\text{Th}$  model. During periods of highest flux and  $f$ -ratio, the agreement was better when  $\text{POC}/^{234}\text{Th}$  and  $\text{PON}/^{234}\text{Th}$  ratios on suspended particles were used. During lower flux periods, the agreement was better when the lower  $\text{C}/^{234}\text{Th}$  and  $\text{N}/^{234}\text{Th}$  ratios found in the sediment traps were used. This is consistent with longer particle residence times and hence preferential C and N loss relative to  $^{234}\text{Th}$  during periods of low export.

(6) Fluxes measured with traps at 150 and 300 m are lower than those estimated from  $^{234}\text{Th}$ . Also, the trap data do not show the large increase in particle export during the first half of May that is indicated by the  $^{234}\text{Th}$  data. Differences between expected and measured trap fluxes are probably due to the familiar problems associated with using traps in the upper oceans (BUESSELER, 1991).

(7) Future studies would benefit from determination of  $^{234}\text{Th}$ , C and N in size fractionated particulate samples. Also, a three-dimensional study of  $^{234}\text{Th}/^{238}\text{U}$  disequilibria would be useful to assess spatial variability.

In order to estimate new production on a global basis, it will be necessary to have a relatively simple technique to estimate vertical export fluxes of carbon and associated nutrients. We believe that  $^{234}\text{Th}$  provides a useful tracer in this regard. It is now possible to measure  $^{234}\text{Th}$  easily at sea (BUESSELER *et al*, 1992), and  $^{234}\text{Th}$  activities respond to biological and physical processes over temporal scales of days to weeks. As an independent constraint on export fluxes, the  $^{234}\text{Th}$  balance avoids many of the complications and assumptions which are inherent in the measurement of vertical fluxes by traps.

*Acknowledgements*—We are indebted to T. Hammar, D. Hirschberg, A. Fler, S. Casso and M. Hartman for their assistance in the sampling and analytical program. Other data collected during the NABE proved critical to our study and were kindly provided prior to publication by many of our colleagues in JGOFS, including J. Martin, H. Ducklow, J. Marra, D. Repeta, D. McGillicuddy, A. Robinson, J. Yoder, R. Williams and C. Goyet. Pre-bloom nutrient and salinity data were provided by S. Honjo and D. Glover. Secretarial assistance was provided by M. Hess. This research was supported by the National Science Foundation (OCE-8817836 and OCE-9016494 to WHOI and OCE-8819544 to SUNY). This is contribution no. 7831 from the Woods Hole Oceanographic Institution and no. 817 from the Marine Sciences Research Center.

## REFERENCES

- ANGEL M. V. (1989) Does mesopelagic biology affect the vertical flux? In *Productivity of the ocean: present and past*, W. H. BERGER, V. S. SMETACEK and G. WEFER, editors, Wiley, New York, pp. 155–173.
- BHAT S. G., B. LAL, RAMA and W. S. MOORE (1969)  $^{234}\text{Th}/^{238}\text{U}$  ratios in the ocean. *Earth and Planetary Science Letters*, **5**, 483–491.
- BROWN O. B., R. H. EVANS, J. W. BROWN, H. R. GORDON, R. C. SMITH and K. S. BAKER (1985) Phytoplankton blooming off the U.S. coast: a satellite description. *Science*, **229**, 163–167.
- BRULAND K. W. and K. H. COALE (1986) Surface water  $^{234}\text{Th}/^{238}\text{U}$  disequilibria: spatial and temporal variations of scavenging rates within the Pacific Ocean. In *Dynamic processes in the chemistry of the upper ocean*, J. D. BURTON, P. G. BREWER and R. CHESSELET, editors, Plenum Press, New York, pp. 159–172.
- BUESSELER K. O. (1991) Do upper ocean sediment traps provide an accurate record of particle flux? *Nature*, **353**, 420–423.
- BUESSELER K. O., J. K. COCHRAN, M. P. BACON, H. D. LIVINGSTON, S. A. CASSO, D. HIRSCHBERG, M. C. HARTMAN and A. P. FLEER (1992) Determination of thorium isotopes in seawater by non-destructive and radiochemical procedures. *Deep-Sea Research*, **39**, 1103–1114.

- BUTMAN C A , W D GRANT and K D STOLZENBACK (1986) Predictions of sediment trap biases in turbulent flows a theoretical analysis based on observations from the literature *Journal of Marine Research*, **44**, 601–644
- CHEN J H , R L EDWARDS and G J WASSERBURG (1986)  $^{238}\text{U}$ ,  $^{234}\text{U}$  and  $^{232}\text{Th}$  in seawater *Earth and Planetary Science Letters*, **80**, 241–251
- COALE K (1990) Labyrinth of doom a device to minimize the “swimmer” component in sediment trap collections *Limnology and Oceanography*, **35**, 1376–1381
- COALE K H and K W BRULAND (1985)  $^{234}\text{Th}$   $^{238}\text{U}$  disequilibria within the California current *Limnology and Oceanography*, **30**, 22–33
- COALE K H and K W BRULAND (1987) Oceanic stratified euphotic zone as elucidated by  $^{234}\text{Th}$   $^{238}\text{U}$  disequilibria *Limnology and Oceanography*, **32**, 189–200
- DEUSER W G (1986) Seasonal and interannual variations in deep-water particle fluxes in the Sargasso Sea and their relation to surface hydrography *Deep-Sea Research*, **33**, 225–246
- DUGDALE R C and J J GOERING (1967) Uptake of new and regenerated forms of nitrogen in primary productivity *Limnology and Oceanography*, **23**, 196–206
- EPPLEY R W (1989) New production history, methods, problems In *Productivity of the ocean present and past*, W H BERGER, V S SMETACEK and G WEFER, editors, Wiley, New York, pp 85–97
- EPPLEY R W and B J PETERSON (1979) Particulate organic matter flux and planktonic new production in the deep ocean *Nature*, **282**, 677–680
- ESAIAS W , G C FELDMAN, C R MCCLAINE and J A ELROD (1986) Monthly satellite-derived phytoplankton pigment distribution for the North Atlantic Ocean basin *Eos*, **68**, 835–837
- FOWLER S W and G A KNAUER (1986) Role of large particles in the transport of elements and organic compounds through the oceanic water column *Progress in Oceanography*, **16**, 147–194
- GARDNER W D (1980a) Sediment trap dynamics and calibration a laboratory evaluation *Journal of Marine Research*, **38**, 17–39
- GARDNER W D (1980b) Field assessment of sediment traps *Journal of Marine Research*, **38**, 41–52
- GIESKES W W and G W KRAAY (1986) Floristic and physiological differences between the shallow and the deep nanophytoplankton community in the euphotic zone of the open tropical Atlantic revealed by HPLC analysis of pigments *Marine Biology*, **91**, 567–576
- GLOVER D M and P G BREWER (1988) Estimates of wintertime mixed layer nutrient concentrations in the North Atlantic *Deep-Sea Research*, **35**, 1525–1546
- GOYET C and P G BREWER (submitted a) Temporal variations of the properties of the carbonate system in the North Atlantic Ocean at 47°N, 20°W I The absorption of atmospheric CO<sub>2</sub> gas by the ocean *Deep-Sea Research*
- GOYET C and P G BREWER (submitted b) Temporal variations of the properties of the carbonate system in the North Atlantic Ocean at 47°N, 20°W II The daily variations of total dissolved inorganic carbon in the upper 150 m *Deep-Sea Research*
- HARGRAVE B T (1985) Particle sedimentation in the Ocean *Ecological Modelling*, **30**, 229–246
- HARRISON W G , T PLATT and M R LEWIS (1987) f-Ratio and its relationship to ambient nitrate concentration in coastal waters *Journal of Plankton Research*, **9**, 235–248
- HONJO S , S J MANGANINI and R KRISHFIELD (1989) Cruise Report JGOFS Leg 1 International Study of the North Atlantic Bloom R/V *Atlantis II* Voyage 119 2 Funchal to Reykjavik March/April 1989 Technical Report WHOI-89-22, Woods Hole Oceanographic Institution, Woods Hole, MA, U S A
- JENKINS W J (1982) Oxygen utilization rates in North Atlantic subtropical gyre and primary production in oligotrophic systems *Nature*, **300**, 246–248
- JENKINS W J and J C GOLDMAN (1985) Seasonal oxygen cycling and primary production in the Sargasso Sea *Journal of Marine Research*, **43**, 465–491
- KAUFMAN A , Y-H LI and K K TUREKIAN (1981) The removal rates of  $^{234}\text{Th}$  and  $^{228}\text{Th}$  from waters of the New York Bight *Earth and Planetary Science Letters*, **54**, 385–392
- KNAUER G A , J H MARTIN and K W BRULAND (1979) Fluxes of particulate carbon, nitrogen, and phosphorus in the upper water column of the northeast Pacific *Deep-Sea Research*, **26**, 97
- KNAUER G A , D M KARL, J H MARTIN and C N HUNTER (1984) *In situ* effects of selected preservatives on total carbon, nitrogen and metals collected in sediment traps *Journal of Marine Research*, **42**, 445–462
- KNUDSON C , W S CHAMBERLIN and J MARRA (1989) Primary production and irradiance data for U S JGOFS (Leg 2) *ATLANTIS II* (Cruise 119-4) 25 April–10 May, 1989 Technical Report LDGO-89-4, Lamont–Doherty Geological Observatory of Columbia University, Palisades, NY, U S A

- KU T-L and M KUSAKABE (1990) Testing biological control of elemental removal in surface ocean with  $^7\text{Be}/^{10}\text{Be}$  and U/Th series isotopes In *Isotopic tracers in JGOFS*, U S JGOFS Report No 12, M P BACON, Chairman and R F ANDERSON, Rapporteur, Report of a U S JGOFS Workshop on Radiochemistry, Woods Hole Oceanographic Institution, 31 May–2 June 1988
- LEE C , S G WAKEHAM and J I HEDGES (1988) The measurement of oceanic particle flux—are “swimmers” a problem? *Oceanography*, **1**, 34–36
- LIVINGSTON H D and J K COCHRAN (1987) Determination of transuranic and thorium isotopes in ocean water in solution and in filterable particles *Journal of Radioanalytical and Nuclear Chemistry, Articles*, **115**, 299–308
- MARTIN J H , S FITZWATER, R M GORDON and W W BROENKOW (1990) Phytoplankton/iron studies during the JGOFS spring bloom study *Eos*, **71**, 81
- MCCAVE I N (1984) Size spectra and aggregation of suspended particles in the deep ocean *Deep-Sea Research*, **31**, 329–352
- MICHAELS A F and M W SILVER (1988) Primary production, sinking fluxes and the microbial food web *Deep-Sea Research*, **35**, 473–490
- MICHAELS A F , M W SILVER, M M GOWING and G A KNAUER (1990) Cryptic zooplankton “swimmers” in upper ocean sediment traps *Deep-Sea Research*, **37**, 1285–1296
- MURRAY J W , J N DOWNS, S STROM, C-L WEI and H W JANNASCH (1989) Nutrient assimilation, export production and  $^{234}\text{Th}$  scavenging in the eastern equatorial Pacific *Deep-Sea Research*, **36**, 1471–1489
- PACE M L , G A KNAUER, D M KARL and J H MARTIN (1987) Primary production, new production and vertical flux in the eastern Pacific Ocean *Nature*, **325**, 803–804
- PEINERT R , B VON BODUNGEN and V S SMETACEK (1989) Food web structure and loss rate In *Productivity of the ocean present and past*, W H BERGER, V S SMETACEK and G WEFER, editors, Wiley, New York, pp 35–48
- PLATT T P and W G HARRISON (1985) Biogenic fluxes of carbon and oxygen in the ocean *Nature*, **318**, 55–58
- ROBINSON A R , D J MCGILLICUDDY, J CALMAN, H W DUCKLOW, M J R FASHAM, F E HOGE, W G LESLIE, J J MCCARTHY, S PODEWSKI, D L PORTER, G SAURE and J A YODER (in press) Mesoscale and upper ocean variability during the 1989 JGOFS bloom study *Deep-Sea Research*
- SACHS P L , T R HAMMAR and M P BACON (1989) A Large-Volume, Deep-Sea Submersible Pumping System Technical Report WHOI-89-55, Woods Hole Oceanographic Institution, Woods Hole, MA, U S A
- SANTSCHI P H , Y-H LI and J BELL (1979) Natural radionuclides in the water of Narragansett Bay *Earth and Planetary Science Letters*, **45**, 201–213
- SIEGEL D A , T C GRANATA, A F MICHAELS and T D DICKEY (1990) Mesoscale eddy diffusion, particle sinking, and the interpretation of sediment trap data *Journal of Geophysical Research*, **95**, 5305–5311
- SLAGLE R and G HEIMERDINGER (1991) North Atlantic Bloom Experiment, April–July 1989 Process Study Data Report P-1, NODC/U S JGOFS Data Management Office, Woods Hole, MA, U S A
- SMALL L F , G A KNAUER and M D TUEL (1987) The role of sinking fecal pellets in stratified euphotic zones *Deep-Sea Research*, **34**, 1705–1712
- SUGIMURA Y and Y SUZUKI (1988) A high-temperature catalytic oxidation method for the determination of non-volatile dissolved organic carbon in sea water by direct injection of liquid sample *Marine Chemistry*, **24**, 105–131
- SUZUKI Y , Y SUGIMURA, E T PELTZER and P G BREWER (1991) DOC and DON concentrations and C/N ratio in the North Atlantic Ocean In *Abstracts, JGOFS North Atlantic Bloom Experiment International Scientific Symposium, Washington, DC (November 1990)*, JGOFS Report No 7, p 22
- TANAKA N , Y TAKEDA and S TSUNOGAI (1983) Biological effect on removal of Th-234, Po-210 and Pb-210 from surface water in Funka Bay, Japan *Geochimica et Cosmochimica Acta*, **47**, 1783–1790
- TOGGWEILER J R (1989) Is the downward dissolved organic matter (DOM) flux important in carbon transport? In *Productivity of the ocean present and past*, W H BERGER, V S SMETACEK and G WEFER, editors, Wiley, New York, pp 65–83
- VERITY P G , D K STOECKER and M E SIERACKI (1990) The impact of grazing by microzooplankton on the North Atlantic spring bloom initial results *Eos*, **71**, 102
- WINGET C L , J C BURKE, D L SCHNEIDER and D R MANN (1982) A self-powered pumping system for *in situ* extraction of particulate and dissolved materials from large volumes of seawater Technical Report WHOI-82-8, Woods Hole Oceanographic Institution, Woods Hole, MA, U S A

## APPENDIX

## A Exact solutions to equations (3), (4) and (5)

We solve equations (3), (4) and (5) assuming that the fluxes  $J$  and  $P$  are constant during a given time interval.  $A_{\text{Th}-1}$  and  $A_{\text{Th}-2}$  are the  $^{234}\text{Th}$  activities at  $t_1$  and  $t_2$ . For dissolved  $^{234}\text{Th}$ , the solution to equation (3) is

$$A_{\text{Th}-2}^{\text{d}} = A_{\text{U}}(1 - e^{-\lambda t}) + A_{\text{Th}-1}^{\text{d}}e^{-\lambda t} - (J_{\text{Th}}/\lambda)(1 - e^{-\lambda t}) \quad (\text{A1})$$

For particulate  $^{234}\text{Th}$ , the solution to equation (4) is

$$A_{\text{Th}-2}^{\text{p}} = \frac{(J - P' + P'^{-1})}{\lambda}(1 - e^{-\lambda t}) + A_{\text{Th}-1}^{\text{p}}e^{-\lambda t} \quad (\text{A2})$$

For total  $^{234}\text{Th}$ , the solution to equation (5) is

$$A_{\text{Th}-2}^{\text{tot}} = A_{\text{U}}(1 - e^{-\lambda t}) + A_{\text{Th}-1}^{\text{tot}}e^{-\lambda t} - \frac{(P' - P'^{-1})}{\lambda}(1 - e^{-\lambda t}) \quad (\text{A3})$$

We rearrange equation (A1) for  $J_{\text{Th}}$  to obtain

$$J_{\text{Th}} = \lambda \left[ \frac{A_{\text{U}}(1 - e^{-\lambda t}) + A_{\text{Th}-1}^{\text{d}}e^{-\lambda t} - A_{\text{Th}-2}^{\text{d}}}{(1 - e^{-\lambda t})} \right] \quad (\text{A4})$$

We rearrange equation (A3) for  $P_{\text{Th}}$  to obtain

$$P_{\text{Th}} = P_{\text{Th}}^{i-1} + \lambda \left[ \frac{A_{\text{U}}(1 - e^{-\lambda t}) + A_{\text{Th}-1}^{\text{tot}}e^{-\lambda t} - A_{\text{Th}-2}^{\text{tot}}}{(1 - e^{-\lambda t})} \right] \quad (\text{A5})$$

When the exact solutions for  $J_{\text{Th}}$  and  $P_{\text{Th}}$  (equations (A4) and (A5)) are calculated from the data in Table 1 and compared to the results using equations (6) and (7) in the text, the difference does not exceed 2%.

B Correction of  $^{234}\text{Th}$  sediment trap fluxes

The measured sediment trap activity,  $A_{\text{Th}}^{\text{trap}}$  ( $\text{dpm m}^{-2}$ ), at the end of a given deployment is a function of the total  $^{234}\text{Th}$  flux,  $F$  ( $\text{dpm m}^{-2} \text{day}^{-1}$ ), and the decay of  $^{234}\text{Th}$  within the trap

$$\frac{\partial A_{\text{Th}}^{\text{trap}}}{\partial t} = F - \lambda A_{\text{Th}}^{\text{trap}} \quad (\text{A6})$$

If the trap flux is assumed constant, and if at  $t = 0$ ,  $A_{\text{Th}} = 0$ , then the solution is

$$A_{\text{Th}}^{\text{trap}} = \frac{F}{\lambda}(1 - e^{-\lambda t}), \quad (\text{A7})$$

where  $t$  is the length of the deployment and  $\lambda$  is the  $^{234}\text{Th}$  decay constant. Rearranging gives

$$F = \frac{\lambda A_{\text{Th}}^{\text{trap}}}{1 - e^{-\lambda t}} \quad (\text{A8})$$

With the deployment time of less than 2 weeks used here, this is equivalent (within 1%) to the linear approximation of decay correcting the measured activity  $A_{\text{Th}}^{\text{trap}}$  ( $\text{dpm m}^{-2}$ ) to the sampling mid-point and dividing by the deployment duration

$$F = A_{\text{Th}}^{\text{trap}} / (te^{-\lambda(t/2)}) \quad (\text{A9})$$